Hybridization in Nanostructured DNA Monolayers Probed by AFM: Theory versus Experiment

Alessandro Bosco, Fouzia Bano, Pietro Parisse, Loredana Casalis, Antonio De Simone, Cristian Micheletti

Supporting Information:

Experimental:

Chemicals: The thiol-modified DNA (P24; SH-$(CH_2)_6$-5'-TAATCGGCTCATACTCTGACTGTA-3') oligomers and non-thiolated complementary strands (T24; 5'-TACAGTCAGAGTATGAGCCGATTA-3') were purchased from Biomers GmbH (Ulm, Germany) as HPLC purified grade and used without further purification. Sodium chloride (NaCl), Tris(hydroxymethyl)aminomethane (Tris) and ethylenediaminetetraacetic acid (EDTA) were purchased from Sigma. Top oligo ethylene-glycol3 terminated alkylthiols (TOEG3, SH-$(CH_2)_{11}$-$(O\text{-}CH_2\text{-}CH_2)_3$-OH) was obtained from Prochimia and fresh solution prepared in pure ethanol (Fluka, purity ≥ 99.8 %) before the experiments. TE buffer (1M NaCl, 10mM Tris, 1mM EDTA, pH 6.9) was prepared using MilliQ water (resistance > 18MΩcm) and filtered through a Millipore filter (GP Express PLUS Membrane, 0.22μm pore size) before use.

Monolayer preparation: For preparing a bio-molecule resistant monolayer on ultra flat gold substrate, a 100 nm thick gold film was deposited on freshly cleaved mica sheets (Mica New York Corp., clear ruby muscovite) at a pressure of about 10^{-5} mbar in an electron-beam evaporator at a rate of 0.1 nm/sec. In this work, Epoxy SU8-100 (negative tone photoresist, MicroChem) was utilized as a solid support. A small drop of SU8-100 was placed over gold slides (few millimeters in size) and then cured to form SU8-100/gold/mica sandwich. The gold-mica interface was disclosed mechanically, and immediately immersed into a freshly prepared 100μM solution of TOEG3 in ethanol for 15 hours at room temperature. The resulting SAM was then rinsed with ethanol and dried under a soft stream of nitrogen.

Preparation of dsDNA: Double-stranded DNA (dsDNA) molecules for nanografting duplexes were prepared by incubation of a 1:3/2 solution of ssDNA and its complementary strands in TE buffer at melting temperature for 10 min. After the incubation, the temperature was allowed to cool down to room temperature and duplexes with final concentrations of 1μM and 2μM were obtained.

AFM: All the Atomic Force Microscope (AFM) experiments were performed by contact-mode XE-100 PARK AFM system (Korea) with a custom liquid cell at room temperature. Standard silicon rectangular cantilevers, (NSC19, MikroMasch, 0.63 Nm^{-1}) and (CSC38/B, MikroMash, 0.03 Nm^{-1}) were utilized for nanografting and imaging, respectively, using the contact-mode AFM. The final radius of curvature of the tips used for the imaging and compressing measurements has been checked by means of Scanning Electron Microscopy measurements and the average value of tenths of tips resulted to be 24±8 nm (see Figure S3)

Nanografting of DNA NAMs and hybridization conditions: The protocol of nanografting has been reported earlier [S1,S2]. Briefly, AFM tip scanned the selected area at relatively large forces (usually in the range of 80-100nN) with a scan rate of 500 nm/sec in the presence of thiolated (ss- or ds-) DNA (1μM (or 2μM) dissolved in a 1:1 mixture of TE buffer and ethanol) solution. This caused TOEG3 molecules from the surface to be replaced locally with thiolated DNA molecules present in the solution. In our previous studies, we have introduced a fabricating parameter that is the ratio, S/A, between the total area (S) that is coated by the tip during nanografting and the area of the patch (A). Practically S/A can be stated as the density of nanografted scanning lines times the tip size at the point of contact with the surface. Therefore, the higher the density of strokes implemented by the tip, the higher the S/A. All the hybridization reactions were carried out at room temperature within an AFM liquid cell for 1 hour. The substrate was washed thoroughly with TE buffer to expunge loosely bound DNA molecules before and after the hybridization reaction.

AFM height and compressibility measurements: Topographic images of resulted Nanografted Assembled Monolayers (NAMs) of DNA were recorded at a minimum force (~ 0.2nN) in TE buffer. In compressibility measurements, the relative heights of (ss- or ds-) DNA NAMs, as a function of the applied load, were collected by gradually increasing the imaging forces from pull-off (low) force (~ 0nN) to high force (~ 2nN).

Preparation of ssDNA SAM and nanografting of TOEG3: freshly cleaved gold substrates

were immersed in a 1M NaCl TE buffer solution with 1 μM thiolated ssDNA for 12-14 hours and subsequently treated in a 1mM mercaptohexanol solution [S3]. TOEG3 has been nanografted into the freshly prepared ssDNA SAMs using a 1:1 mixture of TE buffer and ethanol with 6μM of TOEG3 molecules.

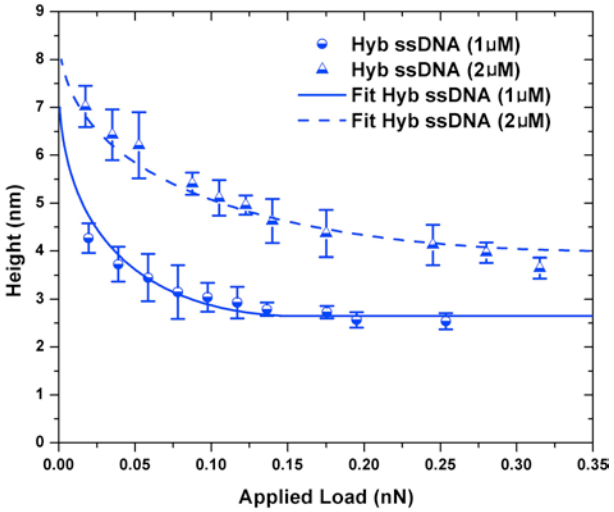

Figure S1: Comparison between experimental (symbol) and computational data (lines) for height vs applied load for ssDNA NAM after hybridization. In order to get an upperbound of the hybridization we fit experimental data with the model for the dsDNA obtaining a surface density equal to $3.6\pm0.4\times10^{12}$molecules cm^{-2} in the 1 μM case and equal to $6.1\pm0.6\times10^{12}$molecules cm^{-2} in the 2 μM case. These values lead to an upperbound of ~30%.

Model of DNA patches:

Here we report a detailed discussion of the terms included in Eq. 1 of the main paper.

Chain Self-avoidance: Each ss- or ds-DNA filament is modeled as a discretized thick chain. The chains consist of segments (virtual bonds) each representing a ds-DNA base-pair or a ss-DNA nucleotide. The segment length, l, is set equal to 0.34nm in both cases. The self-steric hindrance of the chain is taken into account by assigning to each chain a thickness radius equal to Δ. For ss-DNA Δ is equal to 0.45nm while for ds-DNA it is equal to 1.25nm. For the spacer, l is set equal to 0.4nm and Δ=0.225nm. The thickness impacts both on the minimum local and non -local radius of curvature that the chain can attain, and that cannot be smaller than Δ [S4, S5]. This constraint is enforced [S6] by assigning an infinite energy penalty to configurations where the global radius of curvature is smaller than Δ:

$$H_I^{sa} = V_{sa}(\rho_I) \text{ with: } V_{sa}(\rho_I) = \begin{cases} \infty & \text{if } \rho_I \le \Delta_I \\ 0 & \text{if } \rho_I > \Delta_I \end{cases} \qquad \text{(Eq. S1)}$$

where ρ_I is the global radius of curvature for the chain I. Notice that each chain consists of two tethered chains (the ss or ds-DNA and the linker) with different thickness diameter. This heterogeneity has been taken into account when controlling the constraints on the local and non-local radii of curvature.

Bending Rigidity: the contribution of the I-th chain to the bending energy is written as:

$$H_I^{br} = -\varepsilon \sum_{i=2}^{n} \mathbf{t}_i \cdot \mathbf{t}_{i+1} \text{ with: } \begin{cases} \mathbf{t}_i = \mathbf{r}_i - \mathbf{r}_{i-1} \\ |\mathbf{t}_i| = l \end{cases} \qquad \text{(Eq. S2)}$$

where r_i is the position of the i-th vertex in the chain of segments and ε is the bending rigidity. For a chain with no steric hindrance the amplitude of ε is simply related to the persistence length l_p with the following expression $\varepsilon = k_B T l_p$, where k_B is the Boltzmann constant and the temperature T is set to 300K. In the presence of the chain self-avoidance, the effective value of ε

needed to reproduce the decay length of the tangent-tangent correlation at small arclength separations needs to be decreased compared to the previous expression. This tuning was performed through preliminary numerical calculations. The correct ssDNA and dsDNA persistence lengths (respectively equal to ~ 2 nm and ~50nm) were obtained for ε_ssDNA = 0 and ε_dsDNA=147k_BT. For what concerns the alkyl spacer we set ε_spacer = 16k_BT in order to obtain a persistence length equal to 6.5 nm [S7, S8].

Interaction with the surface: the hard-core repulsion between the DNA molecules and the surface is taken into account by forbidding each chain vertex to lie below the plane z=0 which corresponds to the surface. The non-specific attraction of the DNA [S9, S10, S11] with the functionalized gold surface was mimicked by an interaction potential compatible with the order-of-magnitude indications of Gouy-Chapman theory applied to nucleic acids interacting with a moderately-polarized gold-surface (see ref. [38] of the main paper). The effect of the two surface interactions is captured by the following energy term:

$$H_I^{attract} = \sum_{i=2}^{n} V_{attract}(\mathbf{r}_i) \text{ with : } V_{attract}(\mathbf{r}_i) = \begin{cases} \infty & \text{if } r_{i,z} \le 0 \\ -\gamma & \text{if } 0 < r_{i,z} \le \delta \\ 0 & \text{elsewhere} \end{cases} \qquad \text{(Eq. S3)}$$

where δ and γ are, respectively, the range and the strength of the interaction potential. We chose δ=2nm and γ=0.2k_BT in the case of the ssDNA and the alkyl spacer and γ=0.2k_BT in the case of dsDNA. In addition to that, to take into account the finite thickness of the chain we impose a restriction on the maximum angle, up to which the first bond can bend. This is implemented adding this contribution to the Hamiltonian:

$$H_I^{wall} = \sum_{i=2}^{n} V_{wall}(\mathbf{r}_i) \text{with : } V_{wall}(\mathbf{r}_i) = \begin{cases} \infty & \text{if } r_{i,z} \le \max\{1/2, \Delta \sin\theta\} \\ 0 & \text{elsewhere} \end{cases} \qquad \text{(Eq. S4)}$$

where θ is the angle between the vector t_i and a vector normal to the surface.

Mutual self-avoidance of different chains: This excluded volume interaction is enforced by assigning an infinite energy penalty to configurations whenever two chain vertices of different

chains are at a distance smaller that the sum of their thickness radii:

$$H_{I,J}^{beads} = \sum_{i,j=2}^{n} V_{beads}\left(r_{IJij}\right) \text{with}: V_{beads}\left(r_{IJij}\right) = \begin{cases} \infty & \text{if } r_{IJij} \le \Delta_{IJij} \\ 0 & \text{elsewhere} \end{cases} \qquad \text{(Eq. S5)}$$

where r_{IJij} is the distance between the bead i of the chain I and the bead j of the J-chain and Δ_{IJij} is the sum of the radius of the two beads.

Simulation with different number of nucleotides:

We decided also to perform simulations for ss-DNA patches at different number of nucleotides per chain at small applied force per chain (5 pN). In figure S2 are plotted the results. This gives an indication on what happens varying the length of the DNA. Increasing the length of the DNA it increases also the mean patch height of the patch. The dependence of the height on the surface density changes varying the length of the chain.

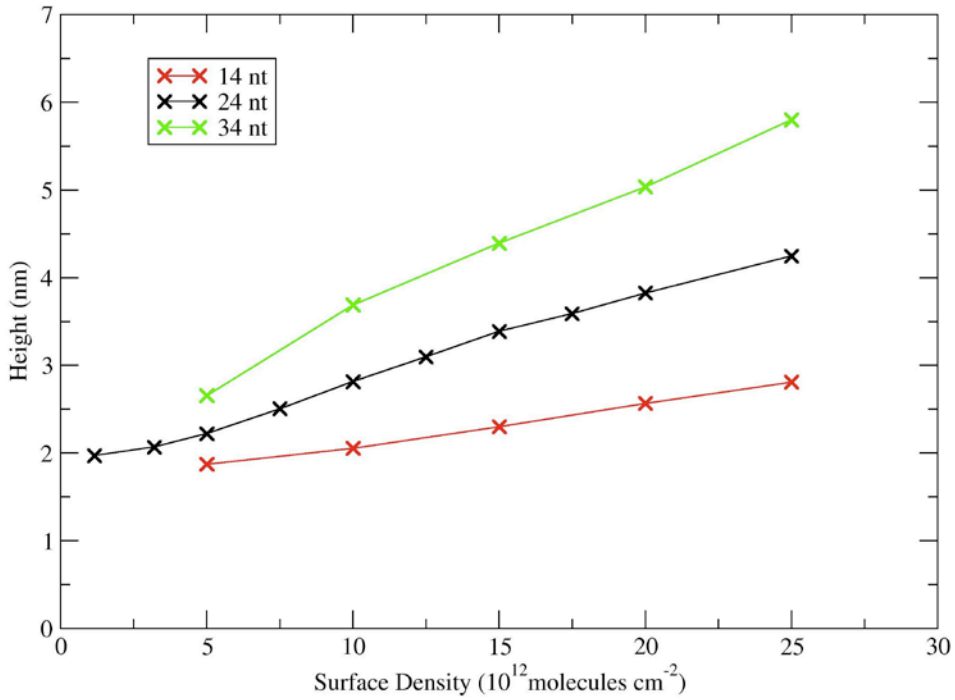

Figure S2: Results of simulations for ss-DNA patches at different number of nucleotides per chain at small applied force per chain (5 pN).

Paraboloid model of the AFM tip:

In cylindrical coordinates, the surface of the tip modeled as a paraboloid can be expressed as,

$$z = h_{tip} + \frac{R^2}{2R_c} \qquad \text{(Eq. S6)}$$

where z is the height from gold surface, h_{tip} the height of the tip apex and R is the distance from the axis of the paraboloid. R_c is the radius of curvature of the paraboloid and is set equal to 25 nm.

With respect to Figure S3, we indicate with h_0 the mean patch height at zero force,

$$h_0 = a_0 + \frac{a_1}{a_2^2} \qquad \text{(Eq. S7)}$$

The penetration depth of the tip is therefore given by $(h_0 - h_{tip})$.

The total load applied to the penetrated tip can be evaluated with a continuum approximation. Using cylindrical symmetry, we integrate the force contributions of the infinitesimal annuli corresponding to section of the paraboloid tip at varying height, z, from the gold surface. For every element of the tip surface, the contribution to the applied load arises both from forces normal (compression of the patch) and parallel to the surface. For sake of simplicity only the contributions normal to surface are considered.

The load of one annulus is equal to the product of the annulus normal surface area, $2\pi RdR$, times the force per unit area of a patch compressed down to height z, that is $\sigma f_{ext}(z)$.

The total applied load, F_{tip}, that the tip experiences can therefore be written as

$$F_{tip} = \int_0^{R_0} 2\pi\sigma R f_{ext}(z) dR \qquad \text{(Eq. S8)}$$

where R_0 is the radius of the paraboloid annulus at $z = h_0$.

Using relations Eq. 3 and Eq. S6 the integral can be evaluated exactly to obtain:

$$F_{tip} = \pi R_c \sigma \left(\frac{2a_1\left(a_0 - h_{tip} + \sqrt{\left(h_{tip} - a_0\right)\left(h_0 - a_0\right)}\right)}{\sqrt{a_1\left(h_{tip} - a_0\right)}} + a_2\left(h_{tip} - h_0\right) \right) \qquad \text{(Eq. S9)}$$

Notice that Eq. S9 requires that $h_{tip} > a_0$. The physical interpretation of this constraint is straightforward because a_0 correspond to the average height of a patch that is uniformly compressed by an "infinite" force (see Eq. 3); consequently the threshold value of the force, F_{max}, beyond which the compressed patch height is a_0 is given by:

$$F_{max} = \pi R_c \sigma \left(2\left(\sqrt{a_1 \left(h_0 - a_0 \right)} \right) + a_2 \left(a_0 - h_0 \right) \right) \qquad \text{(Eq. S10)}$$

as can be easily checked form Eq. S9.

Comparison with experimental data

The experimental data are well fitted by Eq. S9 derived from the coarse- grained model after an optimal choice (fit) of the model patch density σ. The fit was carried out using a least squares procedure with the total applied load F_{tip} and h_{tip} taken respectively as the independent and dependent variable. According to this choice, Eq. S9 was inverted numerically in the range $a_0 < h_{tip} < h_0$ in order to obtain h_{tip} as function of F_{tip}. The surface density σ is then obtained by numerical minimization of the summed square difference between the experimental and computed heights of the patch at various applied load:

$$\chi^2 = \sum_i \frac{\left(h_{i,exp} - h_{i,model} \right)^2}{s_i^2} \qquad \text{(Eq. S11)}$$

where i is running on all the measurement of the patch height, $h_{i,exp}$ and $h_{i,model}$ are respectively the measured experimental height and obtained by the model at given applied load and s_i is the experimental standard deviation on $h_{i,exp}$.

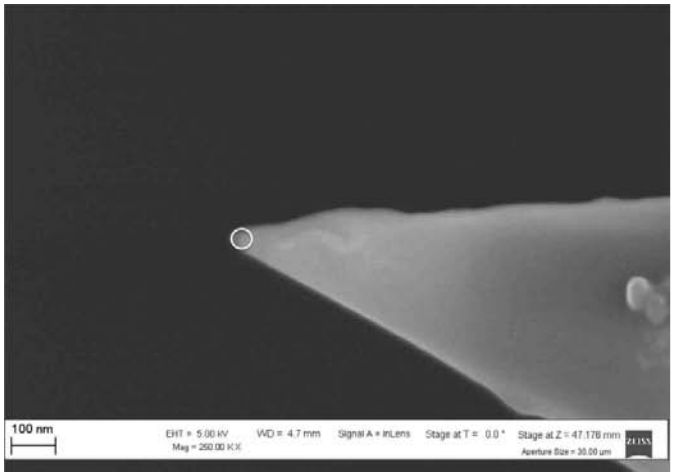

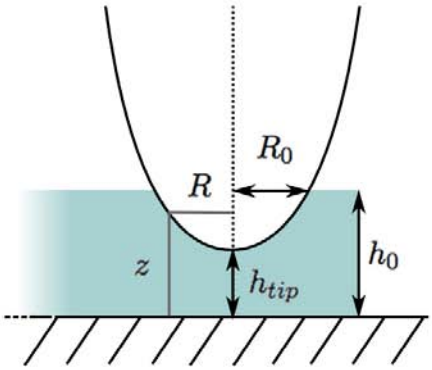

Figure S3: Left panel: Scanning Electron Microscope image of an AFM tip after a height *vs* applied load measure of a DNA patch. The tip has a radius of curvature equal to 23 ± 1 nm (white circle) Right panel: Schematic representation of the paraboloid that mimics the AFM tip penetrating in the DNA patch.

References

[S1] Mirmontaz, E.; Castronovo, M.; Grunwald, C.; Bano, F.; Scaini, D.; Ensafi, A. A.; Scoles, G.; Casalis, L., Nanoletters 2008, 8, 4134-4139

[S2] Castronovo, M.; Radovic, S.; Grunwald, C.; Casalis, L.; Morgante, M.; Scoles, G., Nanoletters 2008, 8, 4140-4145

[S3] Peterson, A. W.; Heaton, R. J.; Georgiadis, R. M., Nucleic Acid Res. 2001, 29, 5163-5168

[S4] Toan, N. M.; Marenduzzo, D.; Micheletti, C. Biophys. J. 2005, 89, 80–86

[S5] Marenduzzo, D.; Micheletti, C. J. Mol. Biol. 2003, 330, 485–492

[S6] Gonzalez, O.; Maddocks, J. H. Proc. Natl. Acad. Sci. USA 1999, 96, 4769–4773

[S7] Yamakawa, H. Annu. Rev. Phys. Chem. 1984, 35, 23–47

[S8] Ramachandran, R.; Beaucage, G.; Kulkarni, A. S.; McFaddin, D.; Merrick-Mack, J.; Galiatsatos, V. Macromolecules 2008, 41, 9802–9806

[S9] Opdahl, A.; Petrovykh, D. Y.; Kimura-Suda, H.; Tarlov, M. J.; Whitman, L. J. Proc. Natl. Acad. Sci. USA 2007, 104(1), 9–14

[S10] Càrdenas, M.; Barauskas, J.; Schillen, K.; Brennan, J. L.; Brust, M.; Nylander ,T. Langmuir 2006, 22, 3294–3299

[S9] Petrovykh, D. Y.; Kimura-Suda, H.; Whitman, L. J.; Tarlov, M. J. J. Am. Chem. Soc. 2003, 125, 5219–5226